

Vol. 14, No. 2 (2025): 623 - 637

http://dx.doi.org/10.23960/jtep-1.v14i2.623-637

JURNAL TEKNIK PERTANIAN LAMPUNG

ISSN 2302-559X (print) / 2549-0818 (online)

Journal homepage: https://jurnal.fp.unila.ac.id/index.php/JTP



Artificial Neural Network Model for Shallot Disease Severity Prediction Using Drone Multispectral Imagery

Angga Firmansyah¹, Mohamad Solahudin^{1,⊠}, Supriyanto¹

¹ Department of Mechanical and Biosystem Engineering, Faculty of Agricultural Engineering and Technology, IPB University, Bogor, INDONESIA

Article History:

Received: 22 July 2024 Revised: 22 October 2024 Accepted: 30 October 2024

Keywords:

Drone, Multi-layer perceptron, Multispectral imagery, Plant disease, Shallot.

Corresponding Author:

mohamadso@apps.ipb.ac.id
(Mohamad Solahudin)

ABSTRACT

Shallot plant diseases can reduce yields by up to 50% of total land area. Currently, shallot plant disease identification relies on direct observation, which is less effective and efficient due to varying intensities of disease and large cultivation areas. This study aims to develop a predictive model for shallot disease severity using multispectral drone imagery, apply Artificial Neural Network (ANN) algorithm to analyze multispectral band data, and evaluate the model's performance. The study used ANN algorithm with multi-layer perceptron regressor, involving following stages such as dataset acquisition, dataset stitching, dataset filtering and feature extraction, model development, and model evaluation. Multispectral data were taken using DJI Mavic 3 Multispectral drone, resulting 696 images per bands that were stitched into orthophoto map. The filtering process of plant objects yielded better model training results compared to unfiltered data. The optimal ANN model structure was identified as 4-6-2-1, with R^2 value of 0.9194 and MAE value of 0.0618. Model testing results demonstrated that using four input bands (G, R, RE, NIR) provided the best performance with R² value of 0.9194, followed by combination of two bands (R, RE) with R² value of 0.8883. This indicated that the R and RE bands were most strongly correlated with shallot disease severity.

1. INTRODUCTION

Shallot (*Allium cepa* L.) is a high value agricultural commodity that provides significant income both local and national communities in Indonesia (Amarillis *et al.*, 2022). According to Kementerian Pertanian (2023), national shallot consumption is 2.96 kg/capita/year or around 825,500 tonnes in 2023. Along with population growth, shallot consumption is projected to increase by 1.47% annually, necessitating a corresponding increase in production. However, plant diseases can cause yield losses exceeding 50% of the total land area (Supyani *et al.*, 2021). Therefore, effective monitoring of shallot diseases is crucial to prevent crop damage and minimize harvest losses (Sari *et al.*, 2017; Solahudin *et al.*, 2015).

Currently, most farmers rely on direct visual inspections or close-room images processed with machine vision for disease monitoring (Kim *et al.*, 2020). Manalu (2023) developed a classification model for shallot diseases using the KNN and CNN algorithms with images taken from a smartphone camera in a closed room. Following this, Purwansya *et al.* (2024) utilized RGB drone images captured directly in shallot fields. However, these methods are less effective for large fields where disease intensity varies, as they are limited to individual detection. In addition to visual detection, plant health can be assessed based on spectral reflectance captured by multispectral sensors cameras (Solahudin & Mutawally, 2020). The use of multispectral camera mounted on drones allows the analysis of plant diseases on a wider scale. The use of multispectral cameras mounted on drones enables the analysis of plant diseases

over large areas. Processing multispectral data with Artificial Neural Network (ANN) algorithms has been demonstrated as effective (Gunardi *et al.*, 2023). The ANN algorithm can be used for complex data processing, multidimensional, and can be implemented on large amounts of data.

This study builds on previous research to analyze shallot disease severity on a grid scale for large fields. The aim is to develop a predictive model for shallot disease severity using multispectral drone imagery, applying an ANN algorithm to analyze multispectral band data and evaluate model performance. The ANN algorithm will explore which combination of multispectral bands has the highest correlation with shallot disease severity. Additionally, the study will analyze the impact of plant object filtering on model performance. A Multilayer Perceptron (MLP) model will be utilized for processing multispectral bands. This disease severity prediction model aims to offer a rapid and accurate monitoring solution for large areas, outperforming conventional methods and individual detection (Messina *et al.*, 2020).

2. MATERIALS AND METHODS

This study was conducted between March and June 2024. Dataset acquisition of shallot plants was taken at Bentak Village, Karangrayung District, Grobogan Regency, Central Java (-7.183272° N; 110.785313° E), as shown in Figure 1. Dataset processing and model development were carried out at the Bioinformatics Engineering Laboratory, Department of Mechanical Engineering and Biosystems, IPB University.



Figure 1. Location of the study area.

Tools and materials used in this research were divided into data acquisition tools and model development tools. The data acquisition process used a DJI Mavic 3 Multispectral drone, gadgets, DJI Pilot 2 software, QField software, ground check marker rope, and Lux Meter. The device used for model development uses computer Intel® Xeon 3.50 GHz with software including Pix4Dmapper, QGIS, Interactive Python Notebook, and Visual Studio Code. The flowchart of the research procedure is shown in Figure 2.

2.1. Dataset Acquisition

Site survey was conducted, then recorded the disease characteristics of shallot fields. Subsequently, image data acquisition was performed using a multi-rotor type drone DJI Mavic 3 Multispectral. Data acquisition was taken at an altitude of 20 m with a Ground Sampling Distance (GSD) of 0.92 cm/pixel. The resolution of multispectral camera on DJI Mavic 3 Multispectral is 5.0 MP with details specifications in Table 1. Dataset were taken every 2 second with front and side overlap between images of 80%. Data collection was carried out in the morning when the angle of incidence of sunlight was more than 30° under bright light conditions. In this condition, the sunlight intensity is effective in obtaining the best multispectral wave reflectance so that it can represent the actual condition of the plant (Merwe et al., 2020).

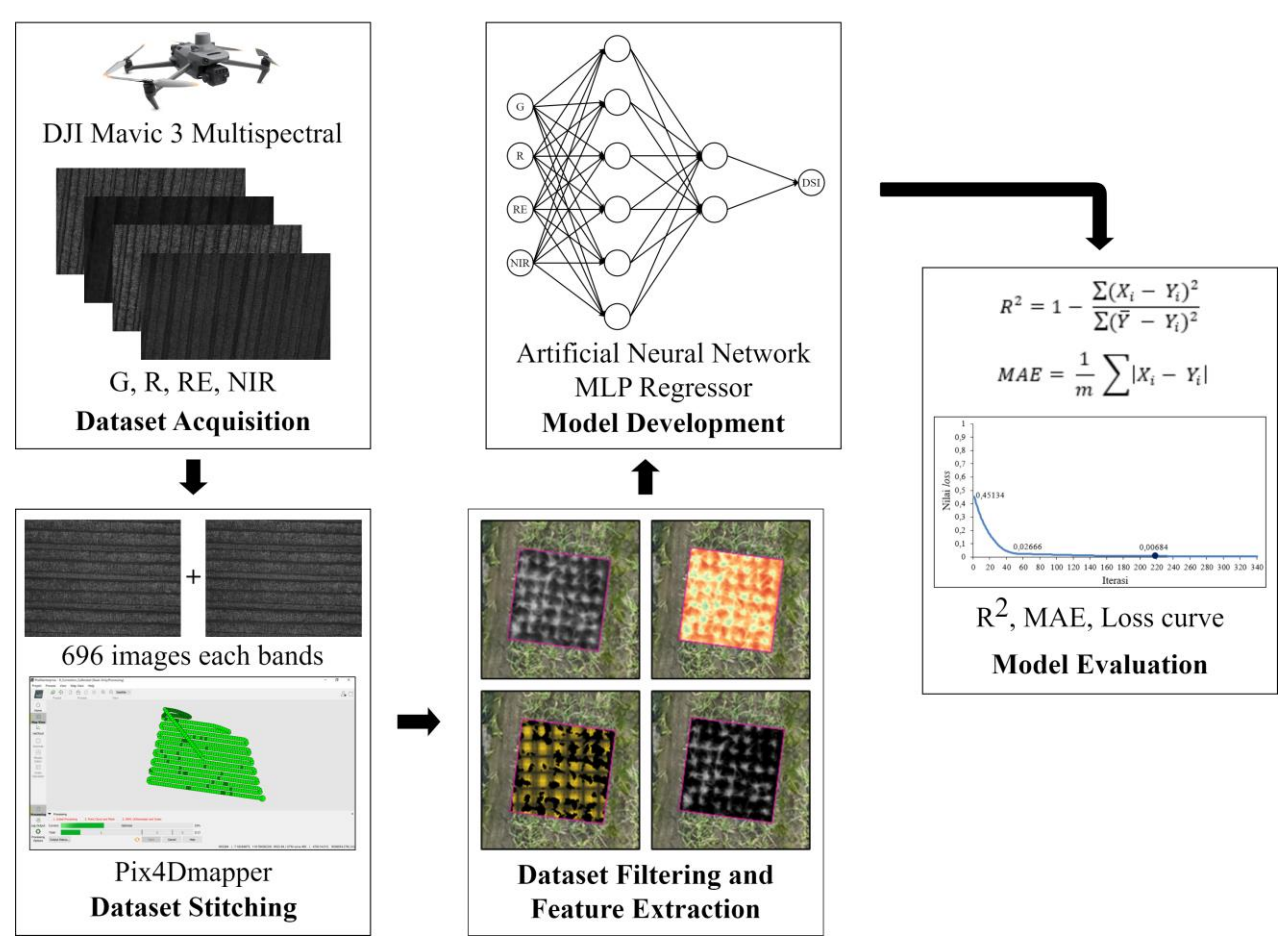


Figure 2. Research workflow of shallot disease prediction model development.

Table 1. DJI Mavic 3M drone multispectral camera specifications

Camera parameter		Specification		
Resolution	5.0 megapixel			
Sensor	1/2,8-inch CMOS			
	Field of view (FOV): 73.9	1° (61.2° x 48.10°)		
Lens	Equivalent focal length: 2	Equivalent focal length: 25 mm		
	Aperture: f/2.0			
	Green (G)	$: 560 \pm 16 \text{ nm}$		
Multispectral camera bands	Red (R)	$: 650 \pm 16 \text{ nm}$		
Multispectral camera ballus	Red Edge (RE)	$: 730 \pm 16 \text{ nm}$		
	Near-infrared (NIR)	$: 860 \pm 26 \text{ nm}$		

Observations of shallot plants infected with the disease used a grid sampling technique (Sholeh & Nurcahyanti, 2023). Validation data collection (ground check) was carried out using QField on a gadget for data recording. The data recorded included the number of shallot plants populations, shallot plants disease, and coordinate location of the data collection point of each sample grid. The research area of 0.45 ha with 44 rectangular beds measuring $1.21 \times 29.26 \pm 0.1 \text{ m}$, 100 grid samples were taken for training data and testing data. The size of the grid sample was adjusted to the width of the land bed, which was $1 \times 1 \text{ m}$. Grid sample data are used to determine the Disease Severity Index (DSI) on each grid sample which is calculated using the following formula (Hersanti *et al.*, 2023):

$$DSI = (n/N) \ 100\%$$
 (1)

where n is the total disease-affected plants per grid, and N is the total plant population per grid.

2.2. Dataset Stitching

Multispectral image datasets taken using drones were grouped according to band data type, namely Green (G), Red (R), Red Edge (RE), and Near-infrared (NIR) images. Furthermore, the image data were stitched using the Pix4Dmapper application as shown in Figure 3. The stitching process produces multispectral orthophoto raster data for each bands in TIFF (Tagged Image File Format) format. An orthophoto is the combined result of a collection of aerial photographs that have been geometrically corrected (Swanda *et al.*, 2021). The data were then analysed for multispectral band filtering and feature extraction using QGIS.

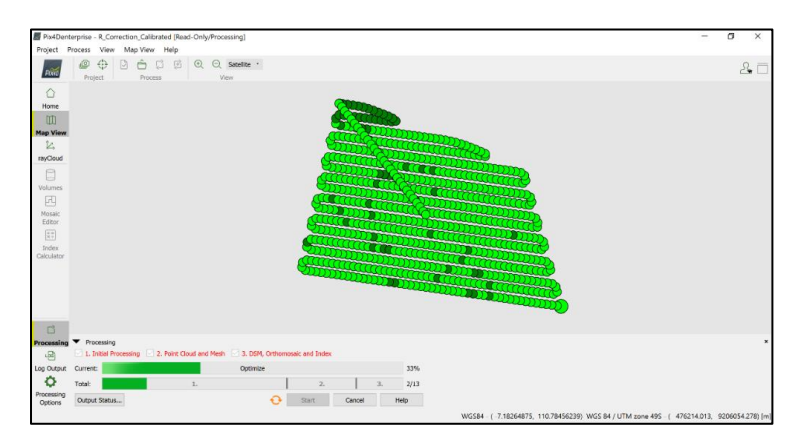


Figure 3. Stitching process for multispectral image data.

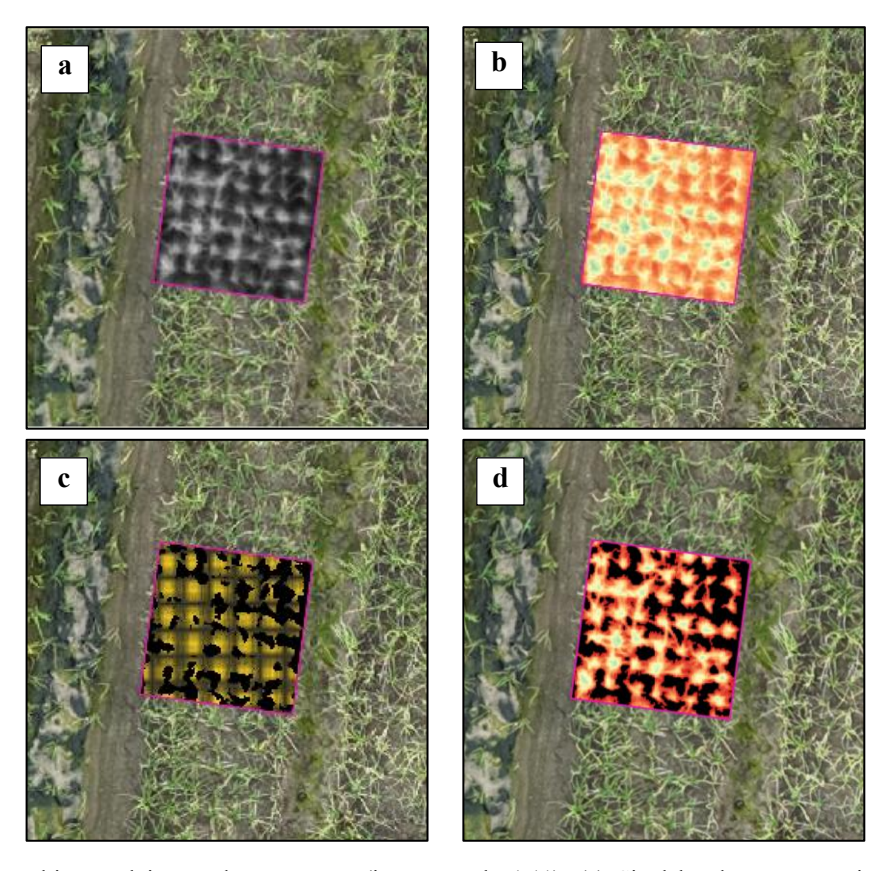


Figure 4. Filtering multispectral image data process (images scale 1:11). (a) Singleband gray raster image; (b) Singleband pseudocolor raster image; (c) Polygon vector image; (d) Filtered raster image of plant object.

2.3. Multispectral Band Filtering and Feature Extraction

The multispectral orthophoto raster data of each band are filtered to separate the shallot plant objects from unwanted objects, such as soil. Data filtering begins with changing the image display (render type) which was previously displayed on a gray scale (singleband gray) (Figure 4a), to a colour scale display (singleband pseudocolour) (Figure 4b). This stage was carried out to determine the range limit between the shallot plant object and the object to be removed. Furthermore, the band value range on the plant object is changed to a value of 1, whereas objects other than plants are changed to a value of 0 using the raster calculator tool. Raster data are converted into polygon-shaped vector data using the raster pixels to polygons tool. Polygons with a value of 0 were removed, resulting in a polygon filter, as shown in Figure 4c. The polygon filter layer was used to separate the shallot plant object in original band layer with the clip raster using the mask layer tool available in raster extraction. The results of filtering the plant objects are shown in Figure 4d.

The next stage is the extraction of multispectral band features from each filtered grid sample. The feature extraction process was carried out using zonal statistics tools on all the multispectral band raster data. Image extraction was carried out to obtain statistical values, including minimum value (min), median value (median), maximum value (max), and average value (mean). These values were used for the ANN model development.

2.4. Dataset Training and Model Evaluation

The machine learning model development was conducted using an Artificial Neural Network (ANN) algorithm. The disease attack rate prediction model was built using the Python programming language in the Interactive Python Notebook environment with a number of supporting libraries, including pandas, numpy, and scikit-learn. The ANN algorithm training method used is the backpropagation method using the multi-layer perceptron regressor (MLP Regressor) function found in the scikit-learn module. Pandas library is used to convert excel extension files to csv, read csv files, change table dimensions, and save training results in excel. Numpy library was used for numerical computation in Python with n-dimensions and various mathematical functions for each parameter. The scikit-learn library was used for data preprocessing, dividing data into training data and testing data, the MLP Regressor model learning process, and model evaluation.

In general, an ANN is composed of input layer, hidden layer, and output layer. There are 400 multispectral band grid sample data (G, R, RE, NIR) as input data from multispectral image feature extraction using zonal statistics tool. The input datasets were transformed using "StandardScaler" from the mean and standard deviation to ensure the data is distributed with a mean of 0 and a standard deviation of 1. Next, the data is divided into training dataset (80%) and testing data (20%) as shown in Figure 5. The model's target output is the intensity of disease attacks, derived from ground check calculations. The normalization equation used as follows:

$$x_{norm} = \frac{x_t - \mu}{s} \tag{2}$$

where x_{norm} is the value after normalization, x_t is the value of the input data, μ is the mean (average) value of the feature, and s is the standard deviation of the feature.

The hidden layers tested in this research started from one, two, and three hidden layers. The number of neurones tested in each hidden layer was 1-21 neurones. The training process continued until it reached the highest R^2 value. The number of hidden layers and neurones was changed to determine the optimum number of each parameter based on the four multispectral bands as the input layer. The sigmoid function is used as the activation function to transfer the input value to the output value which is in the range of 0-1, as in equation 3 (Supriyanto *et al.*, 2019).

$$\sigma(x) = \frac{1}{1 + exp^{-x}} \tag{3}$$

Input layer parameter analysis was conducted to determine the optimum multispectral band combination. The treatment of multispectral band combinations was performed starting from a combination of two, three, and four bands as the input layers. The model training process was performed using the optimum number of hidden layers and neurones in each hidden layer, based on the results of the previous model training. The model training results were evaluated using the coefficient of determination (R²) and Mean Absolute Error (MAE) values, as in equations 4 and 5,



Figure 5. Training data and testing data at the study area.

and the loss curve in the model training process. The R² value shows the correlation of how well the model predicts the target variable, whereas the MAE measures the average absolute error between the value predicted by the model and the actual target value. The model is considered to have good performance if the R² value is close to 1, with an MAE value close to 0 (Satria *et al.*, 2023).

$$R^{2} = 1 - \frac{\sum (X_{i} - Y_{i})^{2}}{\sum (\bar{Y} - Y_{i})^{2}}$$
 (4)

$$MAE = \frac{1}{m} \sum |X_i - Y_i| \tag{5}$$

where X_i is the predicted value, Y_i is the actual value, \overline{Y} is the average of the actual value, and m is the number of data points (Chicco *et al.*, 2021).

3. RESULTS AND DISCUSSION

3.1. Dataset Acquisition and Stitching Result

Observations of the plants indicated symptoms of basal stem rot disease, commonly known as Fusarium wilt. Fusarium wilt, often referred to as "moler", is a prevalent disease affecting shallot crops and is caused by the fungal pathogen Fusarium oxysporum, which can reduce yields by up to 50% of total land area (Prakoso et al., 2016). Visual symptoms observed in the study area included leaf discoloration from pale green to yellow, starting at the tips and progressing toward the base, as well as leaf curling, twisting, drooping, and sudden wilting as shown in Figure 6. These results are in accordance with description of Sholeh & Nurcahyanti (2023). Fusarium oxysporum rapidly proliferates and spreads through soil, necessitating prompt control measures to prevent infection of surrounding plants (Susanti et al., 2016). Advanced stages of infection may occur between 30 days after planting and the end of the harvest period (Supyani et al., 2021). The plants disease severity index is known by direct observations of the total disease-affected plants and the total plant population per grid. The attack value on the grid sample is calculated using equation 1, so that the attack value is obtained in percent units.

The results of the dataset acquisition using DJI Mavic 3M with an altitude of 20 m were 696 drone images of each multispectral band. Image data that are still separate are then stitched using Pix4Dmapper so that orthophoto raster data for each band is obtained, as shown in Figure 7. Orthophoto raster data contains information on the reflectance values of the G, R, RE, and NIR multispectral bands reflected by the object. Based on the image analysis results, it is known that healthy shallot plants, diseased shallot plants, and soil have different multispectral band reflectance values. Based on Figure 8, it is known that healthy plants reflect red waves lower than green, red edge, and NIR waves. This is because the photosynthesis process of plants is strongly influenced by the red spectrum (640 – 700 nm) and the blue

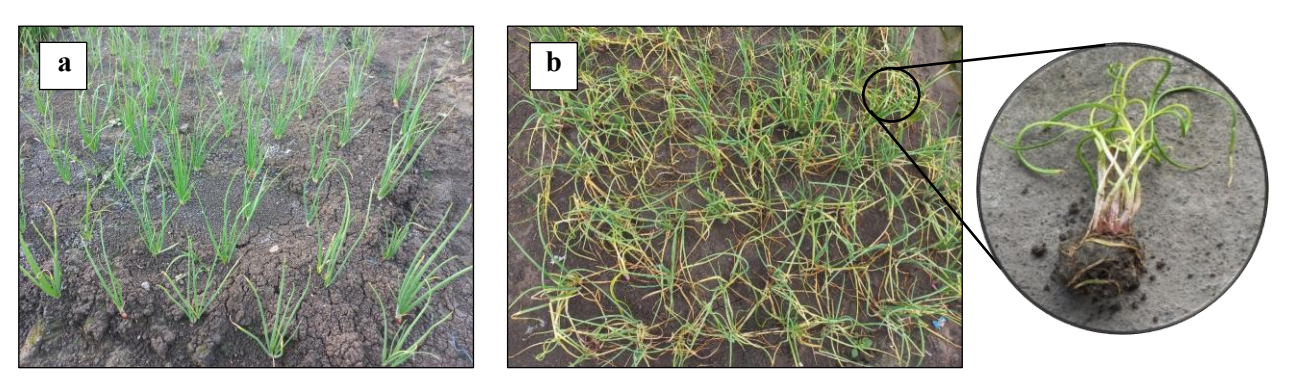


Figure 6. Observation of shallot plants. (a) Healthy shallot plant; (b) Diseased shallot plant.

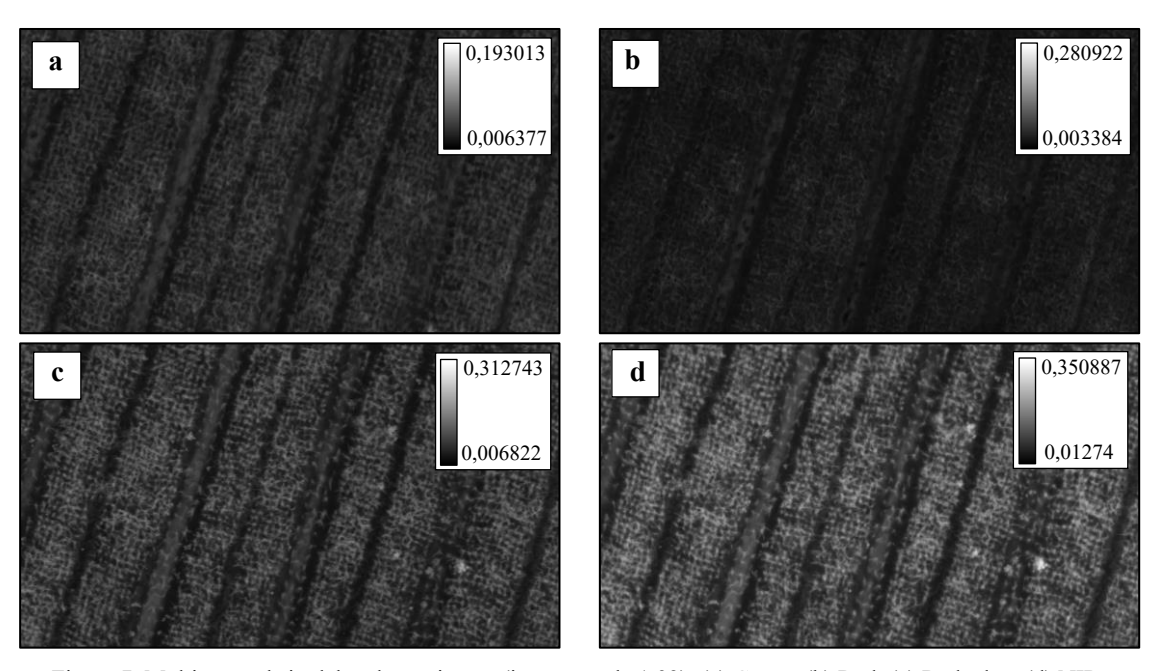


Figure 7. Multispectral singleband gray image (images scale 1:32). (a) Green; (b) Red; (c) Red edge; (d) NIR.

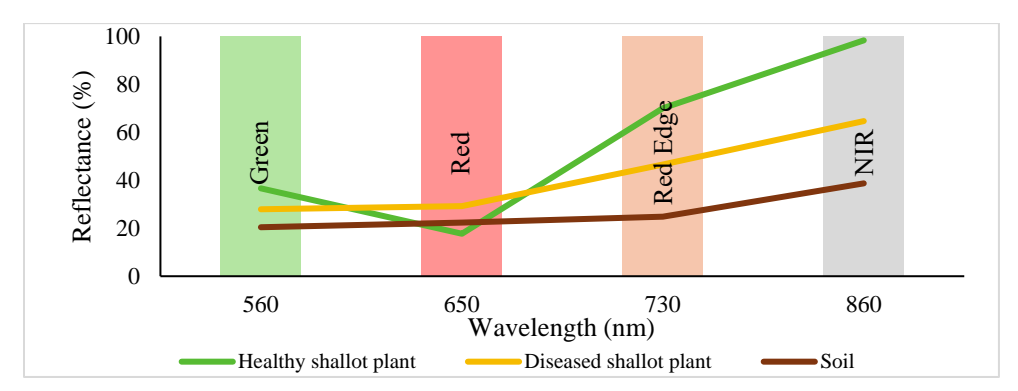


Figure 8. Reflectance values of G, R, RE, NIR bands in healthy shallot plants, diseased shallots, and soil.

spectrum (425 – 490 nm) (Hamim, 2018). The red spectrum is absorbed more by plants for the formation of chlorophyll in the photosynthesis process, but reflects most of the non-visible light (RE and NIR) because of the reflective leaf structure to NIR, especially in the mesophyll layer. Diseased shallot plants reflect lower spectrum of

629

green, RE, and NIR, while exhibiting higher red reflectance compared to healthy plants, indicating reduced efficiency in plant organ function, particularly chlorophyll production. Soil consists of a mixture of mineral particles, organic matter, water, and air that tends to absorb rather than reflect light, so that it has the lowest reflectance value.

3.2. Filtering Process Results of Multispectral Dataset

The filtering process was carried out to remove soil objects, so that obtain only the reflectance value of the shallot plants. The histogram in Figure 9 shows the distribution of reflectance values from the dataset pixels in multispectral image before the filtering process (Figure 9a) and after the filtering process (Figure 9b). The reflectance values shown in Figure 9 are the original values captured by the sensor before the panel calibration and camera correction process on the red edge band as a sample. The results of the multispectral dataset filtering process showed that soil reflectance values lower than the plant reflectance values were successfully removed by the filtering method used. The plant reflectance value is shown by the blue box in Figure 9a and then separated from the soil reflectance value to obtain the plant reflectance value distribution shown in Figure 9b.

After the dataset filtering process, model development was carried out using two types of data, unfiltered and filtered grid sample data. The model training process using these two types of datasets aims to determine the effect of the dataset filtering process on the model performance, then choose the dataset used for model development and analysis. Based on the results of ANN model training using four input variables (G, R, RE, and NIR), the R² value increased from 0.8075 (unfiltered data) to 0.9194 (filtered data). In addition, the MAE value of the model using filtered data was lower (0.0618) than the model using unfiltered data (0.8075) as shown in Table 2. This indicates an increase in model performance with the soil filtering process. Therefore, the filtered dataset was selected for ANN model development.

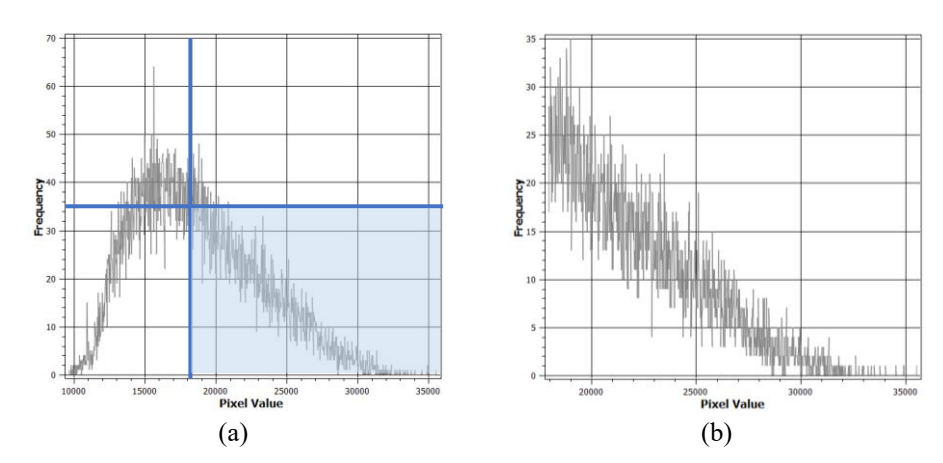


Figure 9. Distribution of reflectance values of dataset pixels in red edge multispectral imagery. (a) Before the filtering process; (b) After the filtering process.

Table 2. Model training results on dataset filtering and non filtering

Dataset	R ² value	MAE value
Non filtering	0.8075	0.8075
Filtering	0.9194	0.0618

3.3. Model Development Results

The ANN machine learning model was developed using the MLP Regressor function available in the scikit-learn module. The input layer consists of four parameters, namely the average value of the Green, Red, Red Edge, and Near-infrared band multispectral images. The number of hidden layers (hl) is determined by testing the number of hidden layers starting from one, two, and three hidden layers. The number of neurons (n) tested in the process of determining

the number of hidden layers is 1-21 in each hidden layer. The output layer in the model training process is the intensity of the disease attack on shallot plants.

The dataset was obtained from the results of multispectral image feature extraction on 100 grid samples. There are 100 grid sample datasets in each multispectral band (G, R, RE, NIR), so that a total of 400 input data and 100 disease attack intensity data are output data. The datasets were transformed using "StandardScaler" from the mean and standard deviation, and then randomly divided into training datasets (80%) and testing datasets (20%) representing each disease attack class. The training process was performed using several model parameters to learn patterns and relationships from the given data. The ANN hyperparameter settings used in the model development are shown in Table 3. Subsequently, the model development was continued with the testing process to test the performance of the ANN model. The determination of hyperparameter values is intended to obtain the best model with high accuracy and low error. The parameter R² and MAE values, as in equations 4 and 5, are used to measure the performance of the ANN model (Chicco et al., 2021).

Table 3. Hyperparameters in the ANN training process

Hyperparameter	Value
Hidden layer	1 – 3
Hidden layer neurons	1 - 21
Activation function	Sigmoid (logistic)
Solver/optimizer	Adam
Learning rate	Constant (0.1)
Momentum	0.5
Maximum iteration	100000
Random state	13
Early stopping	True
Validation fraction	0.2
Tolerance	10^{-15}

Table 4. Model training results on various hidden layers

Number of Hidden Layer	ANN Structure	R ² value	MAE value	Iteration
1	4-6-1	0.8529	0.0719	69
2	4-6-2-1	0.9194	0.0618	340
3	4-6-2-3-1	0.7932	0.0987	73

Four parameters of multispectral band imagery were used to build a prediction model for the level of shallot disease attacks. Based on the results of model training process in one hidden layer, the best model obtained on the ANN structure of 4-6-1 with R² value was 0.8529 and MAE value of 0.0719. Furthermore, the training process is carried out on two hidden layers which shows an increase in the highest R² value of 0.9194 and MAE value of 0.0618. This result shows that the greater number of hidden layers, the higher accuracy of model. The process model training process is again carried out on three hidden layers to obtain the ANN structure in the best model. However, the training results show a decrease in the the highest R² value which is 0.7932 and MAE value of 0.0987. Therefore, the ANN structure of 4-6-2-1 was selected for the next analysis as the proposed model, as shown in Figure 10. The training results of the model on various hidden layers are shown in Table 4.

The ANN model with a structure of 4-6-2-1 consists of four neurons in the input layer, six neurons in the first hidden layer, two neurons in the second hidden layer, and one neuron in the output layer. During the forward propagation process, the input values are processed through each layer until reaching the output. In the first hidden layer, the neuron value z_i is calculated using the equation 6 with weight and bias values as shown in Table 5.

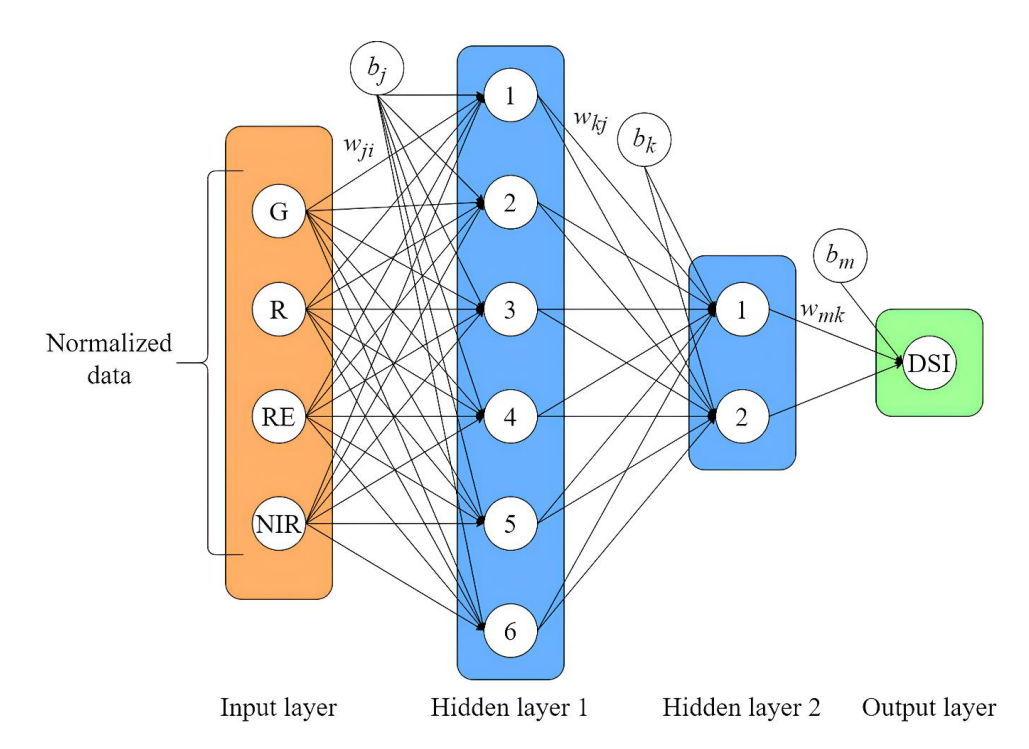


Figure 10. Architecture of the proposed ANN model.

Table 5. Weight and bias values from input layer process to hidden layer 1

Invest lance	Т	Neuron HL 1					
Input layer	Type	1	2	3	4	5	6
Green	weight	-1.6629	-2.9260	0.4160	-1.1393	3.0346	0.0721
Red	weight	-0.6734	0.6692	-0.8545	-2.8537	2.6005	-3.6426
Red Edge	weight	-5.0152	7.3007	-2.3991	0.5930	-2.3764	2.5922
NIR	weight	-2.5155	2.7818	2.0306	0.0423	-7.7058	-1.3772
	bias	1.0213	-2.5713	-3.1765	2.0970	0.2108	-2.8818

Table 6. Weight and bias values from hidden layer 1 process to hidden layer 2

Input nousen III 1	True	Neuron HL 2		
Input neuron HL 1	Type -	1	2	
Neuron 1	weight	1.3418	-1.3306	
Neuron 2	weight	1.5543	-0.9156	
Neuron 3	weight	-1.6840	-0.7314	
Neuron 4	weight	-1.0601	-1.3997	
Neuron 5	weight	1.0763	-1.1184	
Neuron 6	weight	-1.7856	-0.9713	
	bias	-0.3545	-1.3791	

After calculating z_j , the sigmoid activation function is applied to obtain the output a_j . This process is repeated for the second hidden layer, where z_k is calculated using equation 7 with weight and bias values as shown in Table 6, followed by the application of the sigmoid function to obtain a_k value. The output layer calculates z_m using equation 8 with weight and bias values as shown in Table 7, then the final output value (y) is obtained by applying the sigmoid function as in equation 9. Furthermore, the backpropagation process is employed to minimize the error and adjust the

Table 7. Weight and bias values from hidden layer 2 process to output layer

Input neuron HL 2	Туре	Output layer
Neuron 1	weight	0.8549
Neuron 2	weight	0.3595
	bias	0.0517

biases, with the output error calculated from the output layer and propagated back to the hidden layers. Weights and biases are updated using the gradients from backpropagation, and this iterative process continues for up to 100000 iterations, as shown in Table 3, until the model achieves the lowest possible error.

$$z_{j} = \sum_{i}^{4} w_{ji} \cdot x_{i} + b_{j} , \qquad a_{j} = \sigma(z_{j})$$

$$z_{k} = \sum_{i}^{6} w_{kj} \cdot a_{j} + b_{k} , \qquad a_{k} = \sigma(z_{k})$$

$$z_{m} = \sum_{i}^{2} w_{mk} \cdot a_{k} + b_{m} , \qquad a_{m} = \sigma(z_{m})$$
(8)

$$z_k = \sum_{k=0}^{6} w_{kj} \cdot a_j + b_k$$
, $a_k = \sigma(z_k)$ (7)

$$z_m = \sum_{i=1}^{2} w_{mk} \cdot a_k + b_m , \qquad a_m = \sigma(z_m)$$
 (8)

$$\hat{y} = a_m = \sigma(z_m) \tag{9}$$

where z is value of the neuron calculated before applying the activation function, w is weight that connects neurons from the previous layer to the current neuron b is the bias added to enhance the model's flexibility a is the output value after application of the sigmoid activation function, and y is the final output value.

The number of hidden layers that are too large is also not used in training ANN models because it can cause overfitting (Kesuma et al., 2023). Overfitting is a condition when the model learns the training data in too much detail, including noise or random fluctuations in the data or random fluctuations in the data. As a result, the model performs very well on the training data but performs poorly on new data that have never been seen before (testing data). This can occur because the model is too complex with various relative parameters; therefore, the model memorizes the training data rather than finding patterns from the given data.

3.4. Analysis of Multispectral Band Input Parameters

The training process was carried out by testing a combination of several multispectral bands in the input layer with the obtained ANN structure. This aims to analyze the correlation between multispectral bands and the intensity of disease attacks for each combination of input variables. Based on the results of the model training process, it was found that the four-band multispectral input layer had the highest accuracy with an R² value of 0.9194. The combination of the two input band parameters R and RE gives the second-best model results with an R2 value of 0.8883. This shows that the Normalized Difference Red Edge (NDRE) has a strong relationship with the intensity of disease attacks on shallots. NDRE is a plant vegetation index used to measure plant health by comparing red with red edge spectrum reflectance (Davidson et al., 2022). The best combination of three input band parameters is obtained in the combination of bands G, R, and RE with an R² value that is not too different from the combination of bands R and RE, namely 0.8828. This shows that the R and RE bands are input variables with the highest correlation with the level of onion disease attack. The model training results using various multispectral band input scenarios are shown in Table 8.

The R and NIR input band variables also had a strong correlation with the intensity of the disease attack. This is shown in the model training results with input bands R and RE in Table 8, which have an R² value of 0.8506 with an MAE of 0.0817. In addition, the next input band variable consists of R, RE, and NIR, with an R² value of 0.8368 and an MAE of 0.0867. These results indicate that the Normalized Difference Vegetation Index (NDVI) has a strong relationship with the intensity of disease attack in shallots. This is in accordance with the theory of the photosynthesis process, in which plants absorb more of the red and blue light spectrum (visible light), while the RE and NIR spectrum

	-				
Rank	Variables input	Variables exclude	R ² value	MAE value	Iteration
1	G, R, RE, NIR	None	0.9194	0.0618	340
2	R, RE	G, NIR	0.8883	0.0629	41
3	G, R, RE	NIR	0.8828	0.0736	88
4	R, NIR	G, RE	0.8506	0.0817	33
5	R, RE, NIR	G	0.8368	0.0867	48
6	G, R	RE, NIR	0.8255	0.0796	83
7	G, R, NIR	RE	0.8246	0.0922	48
8	G, RE	R, NIR	0.7952	0.1011	43
9	G, NIR	R, RE	0.7823	0.0956	41
10	G, RE, NIR	R	0.7646	0.1094	71
11	RE, NIR	G, R	0.6238	0.1410	50

Table 8. Model training results on various multispectral band input scenarios

(non-visible light) tend to be reflected (Hamim, 2018). Therefore, the lower the red band value and the higher the red edge or near-infrared band value, the healthier is the plant.

3.5. Model Evaluation

Model evaluation was conducted using test data obtained through a data separation process to training and testing dataset. The data separation consisted of 80% training data and 20% testing data from the total ground check data. The dataset included 100 grid samples, from which 20 test data points were randomly selected for data testing each model combination. The ANN model was evaluated based on the R² value to assess accuracy in predicting disease severity index and MAE value to measure prediction error. According to the evaluation results, the best-performing model was a 4-6-2-1 ANN structure using four multispectral input bands: Green, Red, Red Edge, and NIR. The R² value of 0.9194, indicating very high accuracy in the model's predicted disease severity index compared to actual intensity levels. The MAE value of 0.0618 demonstrates a very low prediction error on the test data, as shown in Figure 11. The higher R² value is to 1 and the lower MAE value, the better model performs in predict on the testing data.

The ANN model also evaluated by observing the loss curve to determine how well the model can learn the training data. The loss curve is observed in the best model, namely input bands G, R, RE, NIR with the ANN structure 4-6-2-1. Based on the loss curve in Figure 12, it is known that the loss value in the first iteration is 0.45134, then moves down rapidly to 0.02666 and decreases slowly, approaching 0 at the next iteration. This indicates that the training process is going well. The training process has reached the convergence point at the 219th iteration with the loss value of 0.00684, as shown by the green dot in Figure 12. If the iterations continue, the model performance does not experience significant changes. This means that the model learned as much as possible from the available training data and did not

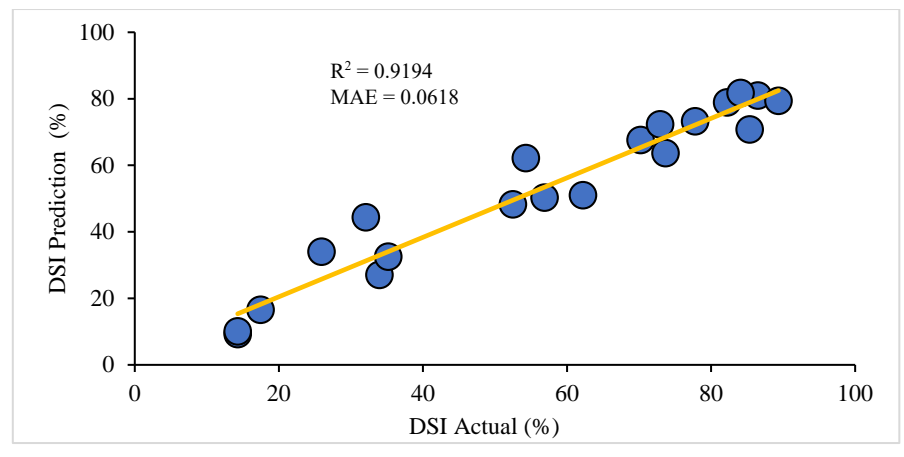


Figure 11. ANN results compared with the target output.

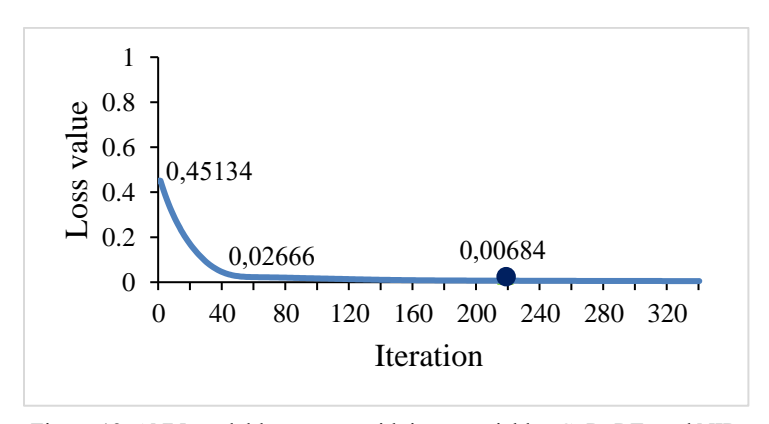


Figure 12. ANN model loss curve with input variables G, R, RE, and NIR.

show significant improvements in the training process. At the converging point, the loss curve tends to decrease towards a stable point, and model parameters such as weights and bias have reached or are close to optimal for good predictions.

Based on the loss curve pattern in Figure 12, it can be observed that the model is fit during the training process, so that it does not experience underfitting or overfitting. The model is said to be underfitting when the loss value is still high, even though the iteration continues. This can happen because the model is too simple to capture the patterns in the data, so it cannot learn the relationship between input parameters properly, and the model has not yet reached the convergent point (Kurniasari & Ammar, 2024). Model overfitting can occur when the loss value continues to increase during the model training process. This can happen because the model is too complex and starts to capture noise or irrelevant details from the training data, so that even though the model shows good performance during the training process, the model's performance is not good enough to predict results with new data.

The implementation of the ANN model can be used to create a map of the level of fusarium disease attacks on shallot plants. The output of the model calculation in the form of disease severity index with a value of 0 - 1, then classified into four classes using percent values and categories referring to the research of Supyani *et al.* (2021) which is shown in Table 9. The model detection results are shown in Figure 13, which is a map representing the level of Fusarium disease attacks in study area. Multispectral image feature extraction was performed on the shallot fields with 2388 detection target grids. Based on the analysis results of the model detection, it is known that the majority of Fusarium diseases are in the high category or class 3, with a total of 45.77% of the study area. The level of disease attacks in the medium category (class 2) is 25.42%, very high category (class 4) is 20.56%, and low category (class 1)

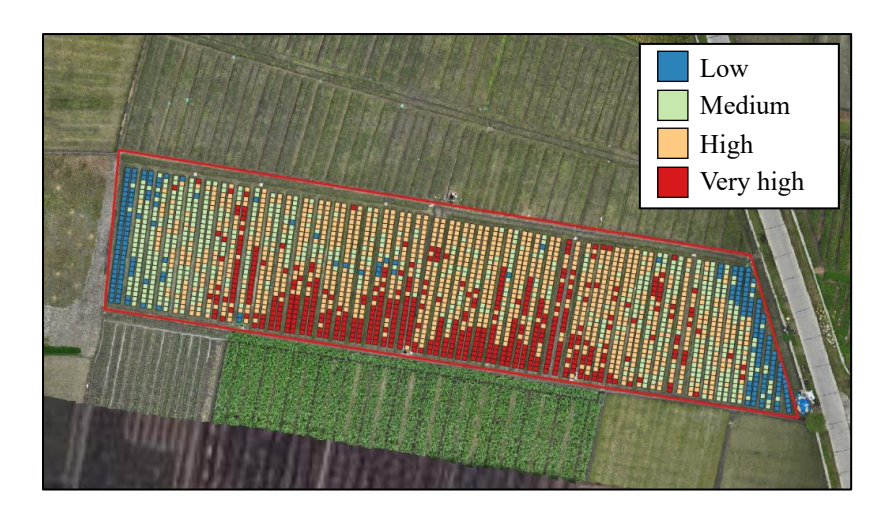


Figure 13. Map of of fusarium disease severity index as a result of ANN model detection.

635

Table 9. Scale on the class of disease attack

Class	Disease severity index (%)	Category
1	1 – 25	Low
2	26 - 50	Medium
3	51 – 75	High
4	76 - 100	Very high

is 8.25%. This shows the need for immediate treatment, such as spraying pesticides on shallot fields, to minimize the decline in crop yields. The map resulting from the detection of disease severity index can be used to distribute different doses during the pesticide spraying process.

4. CONCLUSION

A predictive model for shallot disease severity using multispectral drone imagery has been developed to prevent shallot plant disease attack. The model training process using the MLP Regressor on filtered data of shallot plant objects showed better results compared to unfiltered data. The optimal ANN model structure was identified as 4-6-2-1, with four input bands (G, R, RE, NIR), followed by combinations of two bands (R, RE). This indicated that the R and RE bands were most strongly correlated with shallot disease severity index. The model evaluation results showed an R² value of 0.9194 and an MAE of 0.0618 from the best model, indicating a high level of accuracy in predicting the level of disease attack in shallot plants. The loss curve in the model training process also showed that the model was fit, such that it did not experience underfitting or overfitting. This study suggests that it is necessary to add information of input variables for ultraviolet light reflectance values at various wavelengths to determine their correlation with plant diseases and a larger number of datasets to obtain a model with better accuracy. In addition, increasing the variety and number of datasets is also required to obtain a model with better accuracy.

REFERENCES

Amarillis, S., Solahudin, M., & Sucahyo, L. (2022). The study of shallot seedling from TSS (True Shallot Seed) on LCAC (Low-Cost Aeroponic Chamber). *Earth and Environmental Science*, 1038, 1–7. https://doi.org/10.1088/1755-1315/1038/1/012013

Chicco, D., Warrens, M.J., & Jurman, G. (2021). The coefficient of determination R-squared is more informative than SMAPE, MAE, MAPE, MSE and RMSE in regression analysis evaluation. *PeerJ Computer Science*, 7, 1–24. https://doi.org/10.7717/peerj-cs.623

Davidson, C., Jaganathan, V., Sivakumar, A.N., Czarnecki, J.M.P., & Chowdhary, G. (2022). NDVI/NDRE prediction from standard RGB aerial imagery using deep learning. *Computers and Electronics in Agriculture*, **203**, 107396. https://doi.org/10.1016/j.compag.2022.107396

Gunardi, K., Priandana, K., Hardhienata, M.K.D., Wulandari, & Solahudin, M. (2023). Perbandingan algoritma klasifikasi untuk mendeteksi kebutuhan nitrogen tanaman padi berdasarkan data citra multispectral drone. *Jurnal Ilmu Komputer dan Agri-Informatika*, 10(2), 238–249. https://doi.org/10.29244/jika.10.2.238-249

Hamim. (2018). Fisiologi Tumbuhan 1: Air, Energi, dan Metabolisme Karbon (1st ed.). IPB Press.

Hersanti, Febrianti, N., & Djaya, L. (2023). Effectiveness of nano chitosan and nano silica to suppress the growth of *Fusarium oxysporum*, the cause of twisting disease on shallot. *Jurnal Fitopatologi Indonesia*, 19(6), 265–275. https://doi.org/10.14692/jfi.19.6.265-275

Kementerian Pertanian. (2023). Komoditas Pertanian Subsektor Hortikultura Bawang Merah (1st ed.). Pusat Data dan Sistem Informasi Pertanian.

Kesuma, I.M.S.A., Nugroho, A.S.B., & Aminullah, A. (2023). Pengaruh variasi hidden layer terhadap nilai MAPE pada pengembangan model estimasi biaya menggunakan artificial neural network. *Jurnal Teknik Sipil*, **9**(2), 152–163. https://doi.org/10.31849/siklus.v9i2.14221

Kim, W.S., Lee, D.H., & Kim, Y.J. (2020). Machine vision-based automatic disease symptom detection of onion downy mildew.

- Computers and Electronics in Agriculture, 168(July 2019), 105099. https://doi.org/10.1016/j.compag.2019.105099
- Kurniasari, D., & Ammar, M.N. (2024). Analisis struktur terbaik neural network dengan algoritma backpropagation dalam memprediksi indeks kandungan sulfida (SO2) di Ibu Kota Jakarta. *Jurnal Sistem dan Teknologi Informasi*, *12*(2), 321–329. https://doi.org/10.26418/justin.v12i2.76166
- Manalu, D.R., Sebayang, J., Manullang, H.G. (2023). Klasifikasi penyakit bawang merah melalui citra daun dengan metode K-means. METHOMIKA: Jurnal Manajemen Informatika & Komputersisasi Akuntansi, 7(1), 150-157. https://doi.org/10.46880/jmika.Vol7No1.pp150-157
- Merwe, D., Burchfield, D.R., Witt, T.D., Price, K.P., & Sharda, A. (2020). Drones in agriculture. *Advances in Agronomy*, 162, 1–30. https://doi.org/10.1016/bs.agron.2020.03.001
- Messina, G., Peña, J.M., Vizzari, M., & Modica, G. (2020). A comparison of UAV and satellites multispectral imagery in monitoring onion crop. An application in the 'Cipolla Rossa di Tropea' (Italy). *Remote Sensing*, 12(20), 1–27. https://doi.org/10.3390/rs12203424
- Prakoso, E.B., Wiyatingsih, S., & Nirwanto, H. (2016). Uji ketahanan berbagai kultivar bawang merah (*Allium ascalonicum*) terhadap infeksi penyakit moler (*Fusarium oxysporum f. sp. cepae*). *Jurnal Plumula*, **5**(1), 10–20. http://ejournal.upnjatim.ac.id/index.php/plumula/article/view/773
- Purwansya, Y.G., Solahudin, M., & Supriyanto, S. (2024). Effect of preprocessing and augmentation process in development of a deep learning model for Fusarium detection in shallots. *Jurnal Teknik Pertanian Lampung (Journal of Agricultural Engineering)*, 13(2), 350. https://doi.org/10.23960/jtep-l.v13i2.350-360
- Sari, M.P., Hadisutrisno, B., & Suryanti, S. (2017). Penekanan perkembangan penyakit bercak ungu pada bawang merah oleh cendawan mikoriza arbuskula. *Jurnal Fitopatologi Indonesia*, 12(5), 159. https://doi.org/10.14692/jfi.12.5.159
- Satria, A., Badri, R.M., & Safitri, I. (2023). Prediksi hasil panen tanaman pangan Sumatera dengan metode machine learning. Digital Transformation Technology, 3(2), 389–398. https://doi.org/10.47709/digitech.v3i2.2852
- Sholeh, M.I., & Nurcahyanti, S.D. (2023). Perkembangan penyakit moler (*Fusarium oxysporum f.sp cepae*) pada sentra produksi bawang merah berkala ilmiah pertanian. *Berkala Ilmiah Pertanian*, **6**(2), 56–62. https://doi.org/10.19184/bip.v6i2.35392
- Solahudin, M., & Mutawally, F.W. (2020). Identifikasi Ganoderma pada tanaman kelapa sawit berbasis reflektansi gelombang multispektral. *Jurnal Keteknikan Pertanian*, 7(3), 193–200. https://doi.org/10.19028/jtep.07.3.193-200
- Solahudin, M., Pramudya, B., Liyantono, Supriyanto, & Manaf, R. (2015). Gemini virus attack analysis in field of chili (*Capsicum annuum* L.) using aerial photography and Bayesian segmentation method. *Procedia Environmental Sciences*, 24, 254–257. https://doi.org/10.1016/j.proenv.2015.03.033
- Supriyanto, Noguchi, R., Ahamed, T., Rani, D.S., Sakurai, K., Nasution, M.A., Wibawa, D.S., Demura, M., & Watanabe, M.M. (2019). Artificial neural networks model for estimating growth of polyculture microalgae in an open raceway pond. *Biosystems Engineering*, 177(October), 122–129. https://doi.org/10.1016/j.biosystemseng.2018.10.002
- Supyani, Poromarto, S.H., Supriyadi, Permatasari, F.I., Putri, D.H., Putri, D.T., & Hadiwiyono. (2021). Disease intensity of moler and yield losses of shallot cv. Bima caused by *Fusarium oxysporum f. sp. cepae* in Brebes, Central Java. *Earth and Environmental Science*, 905, 1–5. https://doi.org/10.1088/1755-1315/905/1/012049
- Susanti, D., Mulyadi, & Wiyatiningsih, S. (2016). Karakterisasi isolat-isolat *Fusarium oxysporum f.sp.cepae* penyebab penyakit moler pada bawang merah dari daerah Nganjuk dan Probolinggo. *Plumula*, 5(2), 153–160.
- Swanda, H., Sadjati, E., & Ikhwan, M. (2021). Pemanfaatan teknologi pesawat tanpa awak untuk identifikasi klasifikasi tutupan lahan (Studi kasus: Kawasan Tahura SSH). Seminar Nasional Karya Ilmiah Multidisiplin, 1(1), 157–167.